Liquid Crystals
Publication details, including instructions for authors and subscription information:
http://www.informaworld.com/smpp/title~content=t713926090

Ferroelectric liquid crystal composites based on the porous stretched polyethylene films

Evgeny Pozhidaev[a]; Alexey Bobrovsky[b]; Valery Shibaev[b]; Galina Elyashevich[c]; Maxim Minchenko[a]
[a] P.N. Lebedev Physical Institute of Russian Academy of Sciences, Leninsky prospect 53, Moscow, Russia [b] Faculty of Chemistry, Moscow State University, Leninskie gory, Moscow, Russia [c] Institute of Macromolecular Compounds, Russian Academy of Sciences, 31 Bolshoy pr., Saint Petersburg, Russia

Online publication date: 28 May 2010

To cite this Article Pozhidaev, Evgeny , Bobrovsky, Alexey , Shibaev, Valery , Elyashevich, Galina and Minchenko, Maxim(2010) 'Ferroelectric liquid crystal composites based on the porous stretched polyethylene films', Liquid Crystals, 37: 5, 517 — 525
To link to this Article: DOI: 10.1080/02678291003681386
URL: http://dx.doi.org/10.1080/02678291003681386

Liquid Crystals,
Vol. 37, No. 5, May 2010, 517–525

Taylor & Francis
Taylor & Francis Group

Ferroelectric liquid crystal composites based on the porous stretched polyethylene films

Evgeny Pozhidaev[a], Alexey Bobrovsky[b]*, Valery Shibaev[b], Galina Elyashevich[c] and Maxim Minchenko[a]

[a]*P.N. Lebedev Physical Institute of Russian Academy of Sciences, Leninsky prospect 53, 119991 Moscow, Russia;* [b]*Faculty of Chemistry, Moscow State University, Leninskie gory, 119991 Moscow, Russia;* [c]*Institute of Macromolecular Compounds, Russian Academy of Sciences, 31 Bolshoy pr., 199004 Saint Petersburg, Russia*

(*Received 15 December 2009; final version received 5 February 2010*)

Electro-optically active polymer–liquid crystal composites based on ferroelectric liquid crystals and stretched porous polyethylene films were developed. The alignment of ferroelectric liquid crystals incorporated into the porous polyethylene films with average porous diameter of around 200 nm was observed and studied. It was shown experimentally that these samples containing ferroelectric liquid crystals are flexible electro-optical films exhibiting a saturation electric field near $2{\cdot}10^7$ Vm^{-1} and a response time of about 30 μs under the action of the saturation field. A simple theoretical model of ferroelectric liquid crystal molecules' complete reorientation in electric fields inside pores of the films has been proposed and confirmed experimentally.

Keywords: nano-porous polyethylene; ferroelectric liquid crystals; birefringence; electro-optics

1. Introduction

In recent years, the study of liquid crystals in confined geometry (LCCG) has been an active area of research [1–6]. It is common practice to distinguish two main types of LCCG creation: polymer-dispersed liquid crystals (PDLC) and micro-confined liquid crystals (MLC). PDLC films are usually produced from a suspension of a liquid crystal and a polymer [7–12] in which liquid crystalline droplets with typical sizes of around 1–10 μm are encapsulated. Micro-confinement is considered as a simple insertion of liquid crystals into pre-prepared porous structures of polymer sample [13–15]. It should be mentioned that PDLC and MLC have similar complex multilayer dielectric structures.

The electro-optical behaviour of PDLC, which manifests mainly as electrically controlled modulation of the light scattering (see, for instance, [7, 8]) is very well understood where the liquid crystalline droplet size is not less than 0.5 μm. PDLCs containing droplets of liquid crystal smaller than 100 nm have also been prepared to evaluate their potential as electro-optic materials for waveguide-type devices based on electrically controlled birefringence at negligibly small light scattering [16].

In our present work we have developed an electro-optical media based on LCCG, where the key is the birefringence, rather than scattering, similar to Matsumoto *et al.* [16]. However, we prepared not PDLC but MLC films based on stretched porous polyethylene (PE) with average pore size of about 200 nm, and ferroelectric liquid crystal (FLC).

In our recent research [17–19], this type of oriented porous polymer material was successfully used for the development of new classes of photochromic LC composites with photovariable optical properties, such as dichroism, birefringence, optical density, etc. It was shown that the introduction of nematic mixtures into the PE pores results in perfect orientation of LC director along the stretching axis of PE. Eventually, this orientation leads to the appearance of significant dichroism and birefringence, which can be controlled by the electric field, while the light scattering in the visible spectral range is small. Indeed, the electro-optic effect was observed in 10 μm stretched porous PE films filled with nematic liquid crystals (NLCs), but we were not able to reach the saturation voltage because of electrical breakdown of the film at a voltage of 300–400 V.

Generally, the saturation voltage drastically increases with decreasing liquid crystalline droplet size, a common property and drawback of LCCG [15]. In the present paper we focus our attention on the creation of an electro-optically active LC–PE composite with evident saturation of the electro-optical response through the use of a FLC instead of an NLC.

It should be emphasised that the lowering of the saturation voltage is one of the main problems in the development of electro-optical LC–PE-based composites. If a liquid crystal is placed as one of the layers of the multilayer MLC dielectric structure then the voltage applied to the liquid crystal is always considerably less than the voltage applied to the whole structure. In other words, a very complex voltage divider between polymeric and liquid crystalline sublayers of liquid crystalline–polymeric compositions exists. A dividing ratio of the divider plays a key role in the electro-optics of PDLC and MLC, because the

*Corresponding author. Email: bbrvsky@yahoo.com

ISSN 0267-8292 print/ISSN 1366-5855 online

DOI: 10.1080/02678291003681386
http://www.informaworld.com

voltage applied just to the liquid crystal must be high enough to overcome the threshold voltage and to achieve the saturation voltage of the liquid crystalline layer at corresponding boundary conditions. Therefore we will start our analyses by evaluating the voltage applied to the liquid crystal included in the multilayered MLC dielectric structure.

2. Multilayer dielectric structures including a liquid crystal: theoretical considerations

2.1 Electric field inside elementary multilayer dielectric structure including ferroelectric liquid crystal

As a first approach, let us consider an elementary layer of FLC placed between two dielectric layers (Figure 1). As has been demonstrated (see, for instance, [20, 21]) the FLC possesses the spontaneous polarisation P_s, therefore a depolarisation electric field exists in the multilayer dielectric structure including the FLC layer [22]; see Figure 1.

If the P_s vector is aligned along the y axis (Figure 1), the requirement of the continuity of the dielectric displacement vector D in dielectric multilayer structure yields [23]:

$$\varepsilon_0\varepsilon' E' = \varepsilon_0\varepsilon E + P_s = D, \tag{1}$$

where $E\prime$ and E are the electric field strength in polymeric and liquid crystalline layers, respectively, and ε_0 is the dielectric permittivity of a vacuum. A distribution of the electric potential along the y axis can be written as:

$$2d'E' + dE = V_0. \tag{2}$$

The solution of Equations (1) and (2) has the form:

$$E = E_{FLC} = \frac{\varepsilon' V_0 - 2(P_s/\varepsilon_0)d'}{2\varepsilon d' + \varepsilon' d} = \frac{V_0}{d}\cdot\frac{1-\frac{2P_s d'}{V_0\varepsilon'\varepsilon_0}}{1+\frac{2\varepsilon d'}{\varepsilon' d}}. \tag{3}$$

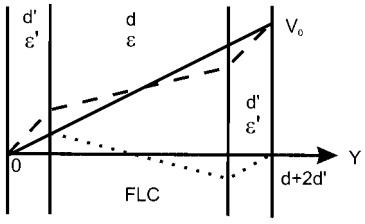

Figure 1. A simple representation of the multilayer dielectric structure including the ferroelectric liquid crystal (FLC) is shown. Here, d is the FLC layer thickness, ε is the FLC dielectric permittivity, and d' and ε' are the thickness and dielectric permittivity of polymeric layers surrounding the FLC, respectively. The solid line represents the distribution of the electrical potential along the y axis if the voltage V_0 is applied to the structure. The electric field E is applied along the y axis. (Reproduced with permission from Lagerwall [21].)

According to our former definitions, E is the electric field tension in the FLC surrounded by two dielectric layers: $E = E_{FLC}$.

If the applied voltage V_0 is switched off, then the so-called depolarisation electric field E^D_{FLC} remains in the FLC. This field direction is always opposite to the field created by the applied voltage (it follows from '-' sign in Equation (3)) and its magnitude can be evaluated from Equation (3) at $V_0 = 0$. So, we have:

$$E^D_{FLC} = \frac{-2(P_s/\varepsilon_0)d'}{2\varepsilon d' + \varepsilon' d}. \tag{4}$$

The depolarisation electric field always exists inside FLC droplets of both PDLC and MLC, even if the external electric field is not applied at all. It partially compensates the external driving electric field which results in an increase of the driving electric field, which is necessary for complete reorientation of FLC molecules under the action of the field.

Let us estimate E^D_{FLC} in FLC placed inside porous PE films, if $d = d' = 200$ nm, $\varepsilon = 5$ (a typical magnitude for liquid crystals), $\varepsilon' = 2.25$ (dielectric permittivity of PE) $P_s = 5{\cdot}10^{-4}$ C m^2 – the spontaneous polarisation of the FLC that was used in our experiments. Taking all necessary parameters listed above for evaluations, we obtain from Equation (4) $E^D_{FLC} = 9.2 \cdot 10^6$ V m^{-1}. According to this very rough estimation, a complete reorientation of the FLC director and, correspondingly, the electro-optical response with a saturation level can be observed if the electric field E applied just to the liquid crystal is not less than E^D_{FLC}.

Consequently, the voltage V_{FLC}, which must be applied directly to the liquid crystal in the pores for observation of the electro-optical response, is not less than:

$$V_{FLC} = E^D_{FLC}\cdot d, \tag{5}$$

where $d = 200$ nm is the averaged porous diameter. The result of this evaluation gives a very rough estimation of the necessary applied voltage $V > V_{FLC} = 1.8$ V. Of course, the voltage applied to the film must be considerably higher, since PE is about half the volume of the film and division of the voltage between PE and liquid crystal is quite sophisticated. We will estimate this division now.

2.2 Electric field inside elementary multilayer dielectric structure including nematic liquid crystal

As is well known, NLCs possess no spontaneous polarisation. Substituting $P_s = 0$ to Equation (3) we obtain the electric field E_{NLC} in the NLC surrounded by two dielectric layers, as shown in Figure 1:

$$E_{NLC} = \frac{\varepsilon' V_0}{2\varepsilon d' + \varepsilon' d} = \frac{V_0}{d} \cdot \frac{1}{1 + \frac{2\varepsilon d'}{\varepsilon' d}}. \quad (6)$$

There is no depolarisation electric field in the NLC if the applied voltage is switched off. The voltage V_{NLC}, applied to the NLC, can be evaluated according to (6) as:

$$V_{NLC} = E_{NLC} \cdot d = \frac{V_0}{1 + \frac{2\varepsilon d'}{\varepsilon' d}}. \quad (7)$$

In fact, we simply have a voltage divider in this case with a division factor:

$$DR_{NLC} = 1 + \frac{2\varepsilon d'}{\varepsilon' d}, \quad (8)$$

as follows from Equation (7). An estimation of the division factor at the same parameters as before: $\varepsilon = 5$, $\varepsilon' = 2.25$, $d = d' = 200$ nm gives us $DR_{NLC} = 5.4$.

2.3 *An apparent division factor of elementary multilayer dielectric structure that includes the ferroelectric liquid crystal*

Starting from Equation (3) we have:

$$V_{FLC} = E_{FLC} d = V_0 \cdot \frac{1 - \frac{2P_s d'}{V_0 \varepsilon' \varepsilon_0}}{1 + \frac{2\varepsilon d'}{\varepsilon' d}}, \quad (9)$$

and we can obtain from Equation (9) the apparent division factor DRA_{FLC} of this structure:

$$DRA_{FLC} = \frac{1 + \frac{2\varepsilon d'}{\varepsilon' d}}{1 - \frac{2P_s d'}{V_0 \varepsilon' \varepsilon_0}}. \quad (10)$$

The DRA_{FLC} magnitude and sign depend on V_0 and P_s. The case $DRA_{FLC} < 0$ means that the depolarisation electric field magnitude is higher than the electric field from the applied voltage V_0. If $P_s \neq 0$ and:

$$V_0 \varepsilon' \varepsilon_0 >> 2P_s d', \quad (11)$$

then $DRA_{FLC} > 0$ and its magnitude tends to minimum, which is equal to DR_{NLS} (see Equation (8)). Equation (11) indicates that for decreasing of $DRA_{FLC} > 0$ we should optimise our composite properties by increasing V_0, ε', d values and by decreasing P_s, d' values.

2.4 *The saturation voltage of multilayer dielectric structures including liquid crystals*

It has previously been shown [15, 24] that the saturation voltage of electro-optical effects in MLC structures strongly depends on a torque, which acts on liquid crystalline molecules in the electric field E_{LC} applied to liquid crystal. The torque is proportional to the volume density of the free energy W_E of interaction between the liquid crystal molecules and the electric field. Amplitude value W_E^A of W_E is expressed for NLC as [25]:

$$W^A_{ENLC} = \frac{\Delta\varepsilon\varepsilon_0 E_{NLC}}{8\pi}, \quad (12)$$

where $\Delta\varepsilon$ is the NLC dielectric anisotropy, while for the FLC inside MLC structure:

$$W^A_{EFLC} = P_s(E_{FLC} - E^D_{FLC}), \quad (13)$$

as we postulated here.

To calculate the dependencies of W^A_{ENLC} and W^A_{EFLC} on the voltage applied to the porous PE film filled in liquid crystals, we made a very rough approximation: the film was replaced by a kind of model multilayered structure, consisting of a sequence of 25 layers, identical to the one shown in Figure 1 with $d = d' = 200$ nm. Under this model, the voltage V applied to the film is defined as: $V = 25\ V_0$. Parameters for evaluations: $\Delta\varepsilon = 20$ for NLC, $P_s = 5 \cdot 10^{-4}$ C m^{-2} for FLC, $\varepsilon = 5$, $\varepsilon' = 2.25$. Equations (3), (4), (6), (12) and (13) were used for evaluations; the result is shown in Figure 2.

For a complete reorientation of the liquid crystal molecules under an electric field in the pores and, consequently, for the achievement of saturation of the electro-optical response, the following conditions should be satisfied:

$$W^A_{ENLC}(V) \geq \frac{2W_Q}{d}, \quad (14)$$

$$W^A_{EFLC}(V) \geq \frac{2W_Q}{d}, \quad (15)$$

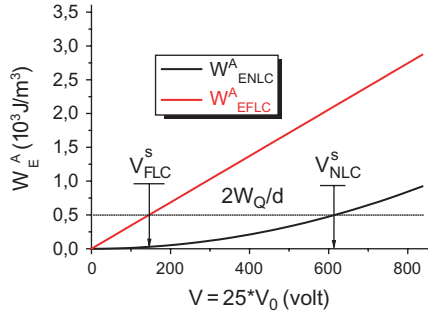

Figure 2. Evaluated dependencies of W^A_{ENLC} and W^A_{EFLC} dependent on the voltage applied to the model of 10-μm thickness multilayer dielectric structures, including polyethylene layers and layers of nematic and ferroelectric liquid crystals.

where W_Q is the anchoring energy coefficient of Rapini potential [26] evaluated experimentally for a pair 'polymer–liquid crystal'. In other words, to achieve saturation it is necessary that the volume density of the free energy W_E of interaction between the liquid crystal molecules and the electric field should exceed the anchoring energy, normalised per unit volume: $2W_Q/d$.

In principle, we can write Equations (14) and (15) suggesting predominantly a spatially uniform distribution of the director of liquid crystal in the pores. That means we neglect the elastic deformation of the director field completely and attribute the switching solely to the competing effects of electric field-induced director reorientation and surface anchoring, assuming a uniform director alignment and reorientation. This assumption is always valid if the distance between the solid surfaces confining the elongated droplets of liquid crystal is less than some critical value [27]. The physical meaning of the last statement follows from the fact that the contribution of the anchoring energy in the free energy is inversely proportional to the distance between the surfaces, but the contribution of elastic energy is inversely proportional to the square of the distance. Here we simply assume that the distance of 200 nm is already critical, therefore neglect the elastic energy. Experimental proof of the validity of this assumption is contained in section 4.2.

A typical value of $W_Q = 10^{-4}$ J m^{-2} was taken from Kiselev *et al.* [28] to calculate the $2W_Q/d$ magnitude. The result of calculation $2W_Q/d = 5{\cdot}10^2$ J m^{-3} is plotted in Figure 2 as a dotted line to find points of intersections of dependencies $W^A_{ENLC}(V)$ and $W^A_{EFLC}(V)$ with $2W_Q/d$ level. Just these intersections indicate the calculated values of saturation voltages: $V^s_{FLC} \geq 145V$ and $V^s_{NLC} \geq 620V$ (see Figure 2). So, calculations show that $V^s_{FLC} << V^s_{NLC}$, even for a case of NLC possessing very high dielectric anisotropy $\Delta\varepsilon = 20$. Taking into account the abovementioned estimations, we have used the FLC mixture for PE-based composite preparation.

3. Experimental details

3.1 General properties of the FLC that was used for filling into the nano-porous PE films

FLC-582 developed in P.N. Lebedev Physical Institute of the Russian Academy of Sciences was used in our experiments. This mixture contains several compounds, whose chemical structure and content (in wt%) are presented in Table 1.

The phase transitions of FLC-582: Cr 2°C SmC* 45°C SmA* 68°C I. The phase transition temperature

Table 1. Chemical structure and content of compounds (%) in FLC-582.

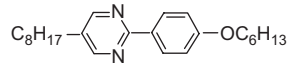	25.8
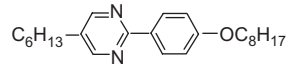	32.2
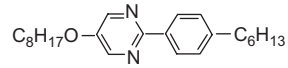	19.3
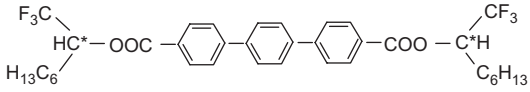	22.7

of the FLC-582 to isotropic phase (68°C) is considerably less than the melting point of the PE porous film (120°C), therefore the permeation of the porous PE film liquid crystal produced in the isotropic phase at $T = 90$°C.

Temperature dependencies of the spontaneous polarisation and rotational viscosity γ_ϕ of FLC-582 are presented in Figure 3. The molecular tilt angle $\theta = 22.5°$ of this FLC at room temperature is the most appropriate for electro-optical measurements.

Let us specify a very low rotational viscosity of the FLC – this parameter is even lower than the rotational viscosity of most NLCs.

A remarkable feature of FLC-582 is the minimal value of γ_φ / P_s ratio. This ratio was selected for two reasons: first, in order to provide a very fast electro-optical response; and second, in order to reduce the frequency dispersion of the saturation voltage, that results in enhancement of $V^s_{FLC}(f)$ with the increasing driving voltage frequency. A parameter of the dispersion is $\gamma_\varphi / P_s d$ [15, 23], therefore diminishing the γ_φ / P_s ratio is very important to shift the dispersion to the higher frequency.

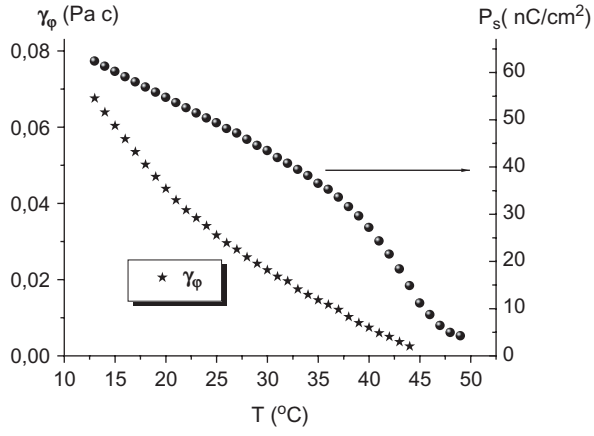

Figure 3. Temperature dependencies of the spontaneous polarisation and rotational viscosity of the FLC-582.

3.2 Preparation of experimental samples

Microporous films of PE were obtained from commercially available PE of low density ($M_w = 1.4\ 10^5$, M_w/M_n = 6–8, $T_m = 132°C$) according to Elyashevitch *et al.* [29]. During extrusion and stretching processes polymer films are deformed, and a porous structure with pores sizes of about 50–500 nm is formed. Pore size distribution was measured by the filtration porometry method, as shown elsewhere [29]. Film thickness was about 10 μm. Figures 4(a) and (b) demonstrate scanning electron microphotography of stretched porous PE film, and pore size distribution. Electron microscopy reveals a large number of microcavities and thin fibres oriented along the stretching direction (Figure 4(a)). As seen from Figure 4(b), the average pore size is relatively small, about 200 nm.

Both PE porous film and FLC were heated to a point higher than the temperature of the FLC phase transition to isotropic phase, but lower than the melting point of the PE film. Porous PE films were filled with the LC mixture under the action of capillary forces at $T = 90°C$, corresponding to the isotropic state of

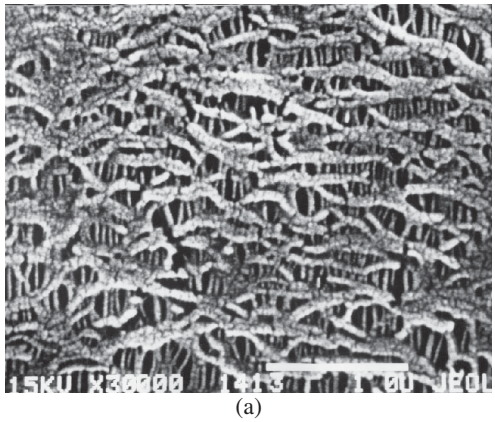

Figure 4. (a) Scanning electron microphotograph of stretched porous polyethylene film used for composite preparation; stretching direction is vertical; white bar corresponds to 1 μm. (b) Through pore size distribution for the same film measured as described in Elyashevitch *et al.* [29].

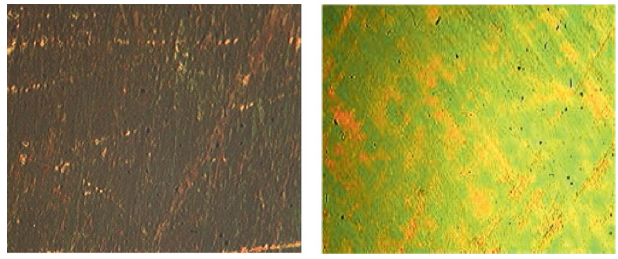

Figure 5. Polarising optical microphotographs showing textures of the porous FLC-PE composite film (10 μm): (a) the angle between the polariser plane and the main direction of porous long axes is 0° (dark state); (b) the angle between the polariser plane and the main direction of porous long axes is 45° (transparent state); the images area is 100 μm × 130 μm (colour version online).

FLC-582. After this procedure the films were cooled down to room temperature and ITO-covered glass was attached to the films. As a result, satisfactory alignment of the FLC molecules inside the porous was achieved (Figure 5).

The light transmission of the dark state (Figure 5(a)) in white light was $T_{0°} \cong 0.015$, while the bright state (Figure 5(b)) was $T_{45°} \cong 0.6$. That means the FLC alignment quality inside the pores of the film is high, with a ratio of light transmission $T_{45°} / T_{0°} = 40$.

3.3 Electro-optical set-up

Electro-optical measurements were carried out using an ordinary electro-optical set-up (Figure 6) based on He–Ne laser (or a source of the white light), LeCroy oscilloscope and rotating table for adjusting of angular position of FLC cells placed between crossed

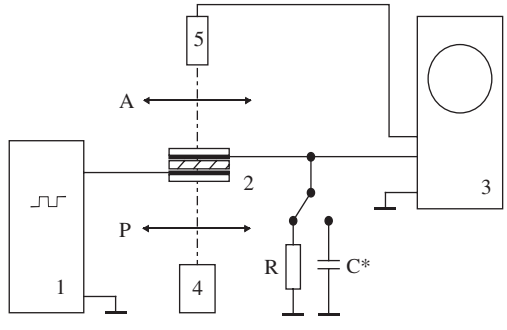

Figure 6. Scheme of the electro-optical set-up: 1 is the voltage generator, 2 is the polyethylene porous film filled with the ferroelectric liquid crystal, sandwiched between two ITO-covered glasses and placed on a rotating table, 3 is the oscilloscope, 4 is the He–Ne laser (or a source of the white light), 5 is the photo-electronic multiplier, A is the analyser, P is the polariser, R is the resistance for registration of the polarisation reversal current, C* is the capacitor for integrating of the polarisation reversal current.

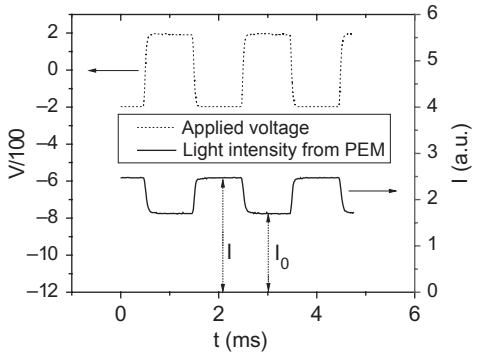

Figure 7. Top – the driving voltage applied to a porous polyethylene film (10 μm) filled with the ferroelectric liquid crystal; bottom – the electro-optical response of the film, placed between two crossed polarisers. The response is measured by a photo-electronic multiplier (PEM) using the set-up presented in Figure 6.

polariser and analyser. A programmed generator WFG-400 was used to generate electrical pulse sequences. A resistance R and a capacitor C* were used to control the polarisation reversal current.

The optical quality was estimated via measurements of the contrast ratio (CR):

$$CR = I/I_0, \tag{16}$$

where I is the maximal light transmission of a cell in 'open' state, and I_0 is the minimal light transmission in 'closed' state, which can be measured with the photo-electronic multiplier (PEM) (Figure 7).

3.4 *Evaluations of birefringence*

Birefringence Δn of porous PE film filled in with FLC was evaluated via measurements of the light transmission spectra of the film placed between crossed polariser and analyser. The spectra were measured with a J&M Tidas diode-array spectrometer.

It is known (see, for instance, Hecht [30]) that the light transmission $T(\lambda)$ of a birefringent plate placed between crossed polariser and analyser, with the angle 45° between the polariser plane and the principle optical axes, is expressed as:

$$T(\lambda) = \sin^2 \frac{\Delta\Phi(\lambda)}{2}, \tag{17}$$

where $\Delta\Phi$ is the phase shift between ordinary and unordinary beams and is expressed as:

$$\Delta\Phi(\lambda) = \frac{2\pi d_p \Delta n(\lambda)}{\lambda}. \tag{18}$$

Here, in Equation (18), λ is the wavelength, and d_p is the birefringent plate thickness. It is evident from Equation (17) that maxima of $T(\lambda)$ magnitudes correspond to:

$$\Delta\Phi = \pi, 3\pi, 5\pi \ldots. \tag{19}$$

while zero of $T(\lambda)$ magnitudes correspond to:

$$\Delta\Phi = 0, 2\pi, 4\pi \ldots. \tag{20}$$

4. Results and discussion

4.1 *Birefringence*

The porous PE film filled with the FLC and placed between the crossed polariser and analyser behaves similarly to a birefringent plate without a considerable contribution of light scattering in the visible spectral range, as can be seen from the transmittance spectrum. It is probable that the light scattering manifests at $\lambda < 500$ nm only (Figure 8), which results in non-zero minima of $T(\lambda)$ in this spectral range.

Nevertheless, positions of maxima and minima of $T(\lambda)$ function do not depend on weak light scattering; therefore we used Equations (17) – (20) and $T(\lambda)$ (Figure 8) to evaluate approximately the birefringence dispersion $\Delta n(\lambda)$ (Figure 9).

A shape of $\Delta n(\lambda)$ function (Figure 9) is similar to the birefringence dispersion of pure FLC, but the magnitude of Δn is approximately two times lower than for the pure FLC mixture at corresponding wavelengths. This can be explained by taking into account the fact that the volume fraction of the FLC mixture in the composite is about 50%, and PE birefringence is much smaller than that of liquid crystal (around $3 \cdot 10^{-3}$ according to our estimations).

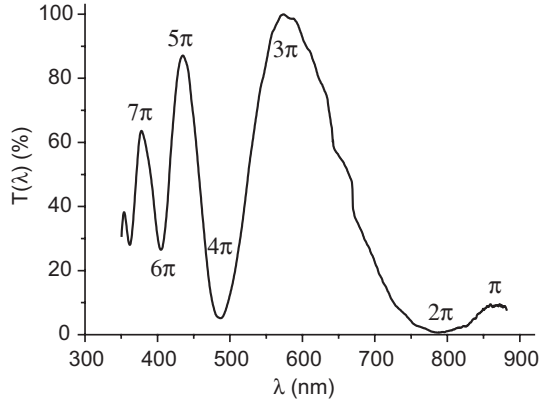

Figure 8. Normalised light transmission of FLC-PE composite film placed between crossed polariser and analyser. The angle between the polariser plane and the stretching direction is 45°.

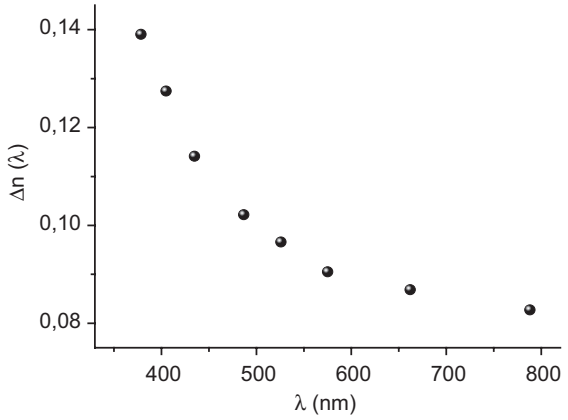

Figure 9. Dispersion of birefringence of the FLC-PE composite film.

4.2 *Electro-optical response*

For investigation of electro-optical properties, the FLC-PE composite films were placed between a crossed polariser and analyser at an azimuthal angle of 22.5° of the stretching direction with respect to the plane of polarisation of the incident light. Electric field application results in a quite remarkable electro-optical response, with very evident 'bright' and 'dark' saturation levels (Figure 10). This means that the response occurs due to electrically controlled modulation of the phase shift between ordinary and extraordinary beams, which appears as a result of complete reorientation of molecules in the electric field.

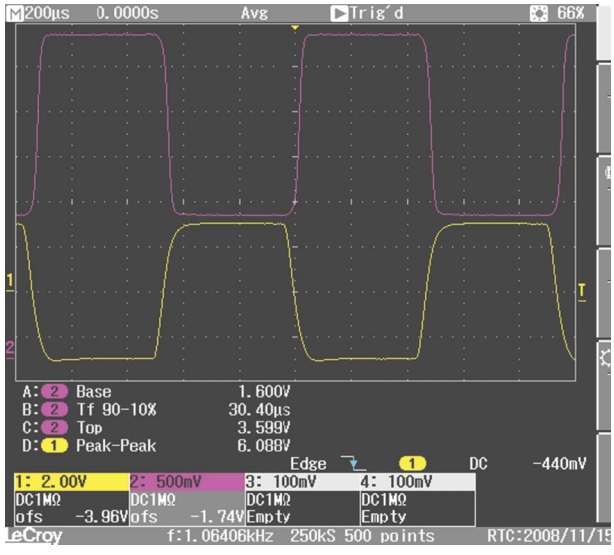

Figure 10. Observation of the electro-optical response of the FLC-PE composite film placed between a crossed polariser and an analyser at an azimuthal angle of 22.5° of the stretching direction with respect to the plane of polarisation of the incident light. The oscilloscope 'LeCroy' included in the set-up (Figure 6) was used: the upper curve on the oscilloscope screen corresponds to the response of the photo-electronic multiplier, and the lower curve corresponds to the applied voltage divided by 50. The electro-optical response was obtained by the modulation of white light passing through the film.

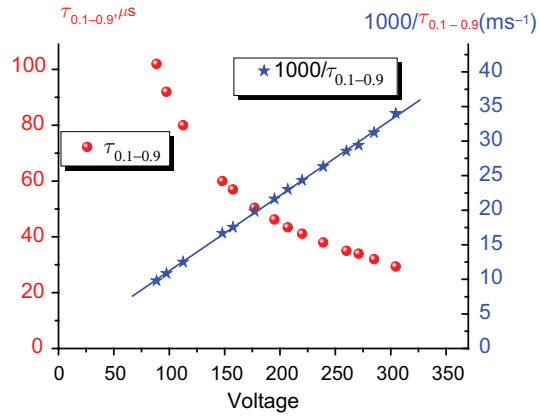

Figure 11. Circles represent the dependence of the electro-optical response time $\tau_{0.1\text{-}0.9}$ of the FLC-PE composite film; asterisks represent dependence of $1000/\tau_{0.1-0.9}$ evaluated from the red curve. The measurements were carried out at an azimuthal angle of 22.5° of the stretching direction with respect to the plane of polarisation of the incident light.

Dynamics of the electro-optical response are illustrated in Figure 11. The response time $\tau_{0.1-0.9}$ is exactly inversely proportional to the applied voltage, as seen from the dependence of $1000/\tau_{0.1-0.9}$ in Figure 11. This kind of proportionality is possible only in the case of spatially uniform director alignment and uniform reorientation in the electric field [31]; therefore, we must completely neglect the elastic deformation of the director field in our analyses. Thus, we have experimental confirmation of the validity of Equations (14) and (15) and, consequently, the true criterion for theoretical calculation of the saturation voltage.

Overall, an ordinary classic behaviour of surface-stabilised ferroelectric liquid crystal mode (SSFLC, [32]) was obtained with the porous stretched PE film filled with FLC. The measured response time is small, and at the highest applied voltage is about 30 µs.

4.3 *Volt-contrast characteristics*

The volt-contrast curve presented in Figure 12 is fairly smooth, therefore the saturation voltage can be only roughly estimated as $V^s_{FLC} \cong 150 - 200V$.

It is worth noting that the measured saturation voltage is quite close to the theoretical estimation obtained in section 2.4, despite the simple approximation and substitution of a complex real structure of porous films on an idealised regular structure in the theoretical model.

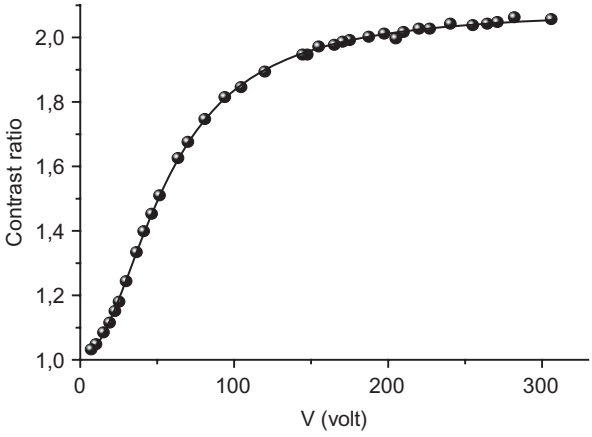

Figure 12. Volt-contrast curve of the FLC-PE composite film; measurements were carried out in white light at room temperature $T = 22°C$.

However, the CR at the electro-optical modulation, defined by Equation (16), is very small – only 2:1 – as shown in Figure 12, and the CR is 20 times lower than a ratio of light transmissions $T_{45°}$ / $T_{0°}$ obtained by the simple rotation of composite film placed between crossed polarisers (see Section 3.2). It is probable that such a low value of CR is associated with the high fraction of very small pores inside PE film filled with 'passive' FLC mixture, because a small value of d prevents any reorientation of FLC molecules, as was shown theoretically in Section 2.4.

5. Conclusion

Electro-optically active polymer–LC composites based on FLC and stretched porous PE films were investigated. An FLC mixture suitable for providing electro-optical behaviour in stretched porous PE films was developed. Alignment of this liquid crystal mixture inside the porous structure of PE was obtained and analysed experimentally. The birefringence of FLC–PE composite films was measured and its high value indicates good orientation of the LC director along the stretching direction of the polymer matrix. It was experimentally shown that the films filled with FLC are flexible electro-optical films, which manifest very evident ordinary SSFLC effects with the saturation electric field near $2{\cdot}10^7$ V m^{-1}. It was found that under application of the saturation voltage the electro-optical response time of the composite films is about 30 μs, and the contrast ratio is 2:1 for the white light.

Acknowledgements

This research was supported by the Russian Foundation of Fundamental Research (Projects 09-03-12234-OFI-M, 08-03-00481-a, 08-07-13554-OFI-TS), and Program COST-D35.

References

[1] Ji, Q.; Lefort, R.; Morineau, D. *Chem. Phys. Lett*. **2009**, *478*, 161–165.
[2] Hung, F.R.; Gettelfinger, B.T.; Koenig, Jr., G.M.; Abbott, N.L.; de Pablo, J.J. *J. Chem. Phys*. **2007**, *127*, 124702.
[3] Blach, J.-F.; Warenghem, M.; Bormann, D. *Vibr. Spectr*. **2006**, *41*, 48–58.
[4] Kancler, A.; Lahajnar, G.; Kralj, S.; Zidansek, A.; Amenitsch, H.; Bernstorff, S. *Mol. Cryst. Liq. Cryst*. **2005**, *439*, 33–42.
[5] Diez, S.; Lopez, D.O.; de la Fuente, M.R.; Perez-Jubindo, M.A.; Salud, J.; Tamarit, J. Ll. *J. Phys. Chem*. **2005**, *109*, 23209–23217.
[6] Lobo, C.V.; Prasad, S.K.; Rao, D.S.S. *Phys. Rev. E* **2005**, *72*, 062701-1-062701-4.
[7] Crawford, G.P.; Zumer, S. *Liquid Crystals in Complex Geometries*; Taylor & Francis Publ.: London, Bristol, 1996.
[8] Doane, I.W. In *Liquid Crystals: Applications and Uses*: Bahadur, B., Ed.; World Scientific Publ., 1990.
[9] Kitzerov, H.S.; Molsen, H.; Heppke, G. *Appl. Phys. Lett*. **1992**, *60*, 3093–3095.
[10] Zyryanov, V.Ya.; Smorgon, S.L.; Shabanov, V.F. *SID-92 Digest* **1992**, *23*, 776–777.
[11] Kundu, S.; Sinha Roy, S.; Pal Majumder, T.; Roy, S.K. *Ferroelectrics*, **2000**, *243*, 197–206.
[12] Smorgon, S.L.; Barannik, A.V.; Zyryanov, V.Ya.; Pozhidaev, E.P.; Andreev, A.L.; Kompanets, I.N.; Ganzke, D.; Haase, W. *Mol. Cryst. Liq. Cryst*. **2001**, *368*, 207–214.
[13] Rosanski, S.A.; Stannarius, R.; Kremer, F. *IEEE Trans. Dielectr. Electr. Insul.* **2001**, *8*, 488–493.
[14] Rosanski, S.A.; Stannarius, R.; Kremer, F.; Diele S. *Liq. Cryst.* **2001**, *28*, 1071–1083.
[15] Pozhidaev, E.; Haase, W. *Relaxation Phenomena – Liquid Crystals, Magnetic Systems, Polymers, High-T_C Superconductors, Metallic Glasses*; Springer: Berlin, 2003; pp 376–400.
[16] Matsumoto, S.; Sugiyama, Y.; Sakata, S.; Hayashi, T. *Liq. Cryst*. **2000**, *27*, 649–655.
[17] Bobrovsky, A.; Shibaev, V.; El'yashevitch, G.; Shimkin, A.; Shirinyan, V. *Liq. Cryst*. **2007**, *34*, 791–797.
[18] Bobrovsky, A.; Shibaev, V.; Elyashevitch, G.; Rosova, E.; Shimkin, A.; Shirinyan, V.; Bubnov, A.; Kaspar, M.; Hamplova, V.; Glogarova, M. *Liq. Cryst*. **2008**, *35*, 533–539.
[19] Bobrovsky, A.; Shibaev, V.; Elyashevitch, G. *J. Mater. Chem*. **2008**, *18*, 691–695.
[20] Meyer, R.B.; Libert, L.; Strzelecki, L.; Keller, P. *J. De Phys. Lett*. **1975**, *36*, L-69–L-71.
[21] Lagerwall, S.T. *Ferroelectric and Antiferroelectric Liquid Crystals*; WILEY-VCH Verlag: Berlin, 1999.
[22] Yang, K.H.; Chieu, T.C.; Osofsky, S. *Appl. Phys. Lett.* **1989**, *55*, 125–127.
[23] Blinov, L.M.; Palto, S.P.; Pozhidaev, E.P.; Bobilev, Yu.P.; Shoshin, V.M.; Andreev, A.L.; Podgornov, F.V.; Haase, W. *Phys. Rev. E* **2005**, *71*, 051715.
[24] Pozhidaev, E.P.; Smorgon, S.L.; Andreev, A.L.; Kompanets, I.N.; Shin, S.T. *Trends Optics Photonics Ser*. **1997**, *14*, 94–101.
[25] Chigrinov, V.G. *Liquid Crystal Devices: Physics and Applications*; Artech House: Boston, London, 1999.

[26] Rapini, A.; Papoular, M.J. *J. Phys. (France) Colloq.* **1969**, *30*, C4–C54.
[27] Kaznacheev, A.V.; Bogdanov, M.M.; Sonin, A.S. *J. Experiment. Theor. Phys.* **2003**, *97*, 1159–1167.
[28] Kiselev, A.D.; Chigrinov, V.G.; Pozhidaev, E.P. *Phys. Rev. E* **2007**, *75*, 061706.
[29] Elyashevitch, G.K.; Kozlov, A.G.; Rozova, E.Yu. *Vysokomol. Soedin. A* **1998**, *40*, 956–963 (in Russian).
[30] Hecht, E. *Optics*, 4th edition; Addison Wesley, 2002.
[31] Barnik, M.I.; Baikalov, V.A.; Chigrinov, V.G.; Pozhidaev, E.P. *Mol. Cryst. Liq. Cryst.* **1987** *143*, 101–112.
[32] Clark, N.A.; Lagerwall, S.T. *J. Appl. Phys.* **1980**, *36*, 899–903.